Journal of Atmospheric and Solar-Terrestrial Physics 73 (2011) 544–550

Contents lists available at ScienceDirect

Journal of Atmospheric and Solar-Terrestrial Physics

journal homepage: www.elsevier.com/locate/jastp

# Mie lidar and radiosonde observations at Gadanki (13.5°N, 79.2°E) during sudden stratospheric warming of 2009

S. Sridharan [a,*], K. Raghunath [a], S. Sathishkumar [b], D. Nath [a]

[a] National Atmospheric Research Laboratory, Gadanki, Andhra Pradesh, India
[b] Equatorial Geophysical Research Laboratory, Indian Institute of Geomagnetism, Tirunelveli, Tamilnadu, India

ARTICLE INFO

*Article history:*
Received 9 February 2010
Received in revised form
9 November 2010
Accepted 11 November 2010
Available online 21 November 2010

*Keywords:*
Stratospheric warming
Meridional circulation
Tropical convection
Cirrus clouds

ABSTRACT

During a major sudden stratospheric warming event (21–27 January 2009), Mie-lidar observations at Gadanki (13.5°N, 79.2°E) show persistent occurrence of cirrus clouds. Outgoing long-wave radiation averaged for 70°E–90°E, decreases to a low value (170 W/m$^2$) on 27 January 2009 over equator indicating deep convection. The zonal mean ERA-Interim data reveal large northward and upward circulation over equatorial upper troposphere. The latitude–longitude map of ERA-Interim zonal mean potential vorticity (PV) indicates two tongues of high PV emanating from polar latitudes and extending further down to equator. Radiosonde observations at Gadanki show the presence of ~40% relative humidity at 11–13 km and lower tropopause temperature. It is inferred that the tropical circulation change due to PV intrusion leads to deep convection, which along with high humidity and low tropopause temperature leading to the formation of persistent cirrus clouds, the occurrence frequency of which is normally less during winter season over Gadanki.



## 1. Introduction

Sudden stratospheric warming (SSW) is a dramatic event in the winter polar middle atmosphere, involving considerable changes of temperature, wind and circulation within a short span of time. For the formation of the SSW event, Matsuno (1971) proposed a theory, which has been widely accepted, is that the warming occurs due to convergence of heat flux carried by planetary waves at higher latitudes and subsequently induces mean upward winds. These vertical motions accompany mean meridional flow, which due to Coriolis force induces westward acceleration on the existing eastward polar circulation and decelerate them. When the planetary flux is larger, the westward acceleration may even change the circulation, in which case, the warming event is considered as a major event.

The meridional circulation associated with the sudden warming can induce upwelling in the equatorial region and produce a cooling in the equatorial lower stratosphere. The association of cooling in the equatorial latitudes was first revealed by NIMBUS satellite observations (Fritz and Soules, 1970). According to downward control principle of Haynes et al. (1991), the convergence/divergence of the meridional circulation can induce vertical flow below. The idealized general circulation model experiment of Thuburn and Craig (2000) demonstrated that the stratospheric meridional circulation change can affect the diabatic heating rate of convection in the equatorial troposphere. Yulaeva et al. (1994) showed that tropical tropopause temperature can be influenced by eddy fluxes in the extra-tropical winter stratosphere, which is consistent with the downward control principle of Haynes et al. (1991).

There have been only a few observational reports on how a major SSW event influences tropical troposphere. Kodera and Yamada (2004) observed that a major warming of the southern hemisphere in September 2002 produced a north-south seesaw of tropical convection activity. They also found that the tropical convection became active and shifted toward the southern hemisphere following the equatorial cooling. Kodera (2006) also noted similar features resulting from the composite analysis of twelve major warming vents occurred at high latitude northern hemisphere. Eguchi and Kodera (2007) observed persistent tropical cirrus clouds due to low temperature formed by upwelling associated with the southern hemisphere SSW event.

In this study, we report mainly radiosonde observations of atmospheric parameters, namely, wind velocity, relative humidity and temperature and Mie-lidar observations of scattering ratio at Gadanki, a low latitude site, over a time period prior to and during a major SSW event of 2009.

## 2. Observations and data analysis

### 2.1. Radiosonde observations

GPS radiosonde balloons have been launched daily at Gadanki since April 2006 at 1200 UT. The atmospheric parameters, namely,

* Corresponding author. Tel.: +91 8585 272124; fax: +91 8585 272018.
*E-mail address:* susridharan@narl.gov.in (S. Sridharan).

1364-6826/$ - see front matter © 2010 Elsevier Ltd. All rights reserved.
doi:10.1016/j.jastp.2010.11.016

temperature, pressure, relative humidity and horizontal wind are obtained with a height resolution of 5 m from surface to about 30 km. In the present paper, the parameters averaged for 100 m are used for the analysis. The horizontal winds, temperature and relative humidity are measured with an accuracy of 0.5 m/s, 0.5 K, and 5%, respectively (Nath et al., 2010).

### 2.2. Mie-lidar observations at Gadanki

The elastic backscatter Mie-lidar system has been operational at Gadanki since the year 1998. The transmitter part consists of newly replaced Nd:YAG pulse laser source at the second harmonic of 532 nm with a maximum energy of about 600 mJ per pulse with a repetition rate of 50 Hz. The receiver consists is a Schmidt Cassegrain telescope with a diameter of 35 cm and the field of view of 1 mrad. A photo multiplier tube with a narrowband interference filter centered at 532 nm (FWHM of 1.13 nm) is used in front of the polarization beam splitter, which splits the beam into cross- and co-polarized components with comparable gains. The photon counting signals are sent to an MCS-Plus channel for signal analysis. The lidar system is a monostatic biaxial system and is optically aligned to heights greater than 8 km so that low level clouds and aerosols would not interfere with the observation. The dwell time of the counting system is 2 μs, which corresponds to an altitude resolution of 300 m.

The lidar detects atmospheric backscatter from both aerosol and molecules. In order to separate aerosols from molecules inversion methods are adopted. The noise and range-corrected photon counts are normalized with the MSIS model atmosphere air density profile corresponding to 15°N, typically in the altitude range of about 35 km where backscattered photons due to aerosols are either insignificant or nil.

From the reference altitude $z_m$ (=35 km) where the backscattering contribution is mainly due to air molecules, the top to bottom integration is performed. The total backscattering coefficient $\beta_z$ obtained using the top to bottom inversion algorithm proposed by Klett (1985) can be written as

$$\beta_z = \frac{\exp(S - S_m)}{\dfrac{1}{\beta_m} + 2\int_z^{z_m} \dfrac{\exp(S-S_m)}{B_a} dz}$$

where $S$ and $S_m$ are logarithm of the range-corrected photon counts at any altitude $z$ and the reference altitude $z_m$, respectively. $\beta_m$ corresponds to the Rayleigh backscattering coefficient at altitude $z_m$. Rayleigh backscattering coefficients are estimated from pressure and temperature profiles using MSIS model values at 15°N. $B_a$ (sr$^{-1}$) is the ratio between aerosol backscattering and extinction coefficients and is taken as a constant value of 0.019 with altitude (Ramachandran and Jayaraman, 2003), in which case, the solution is similar to that obtained by Fernald (1984). The calculated total backscattering coefficient $\beta_z$ is further used to calculate the Scattering Ratio (SR),

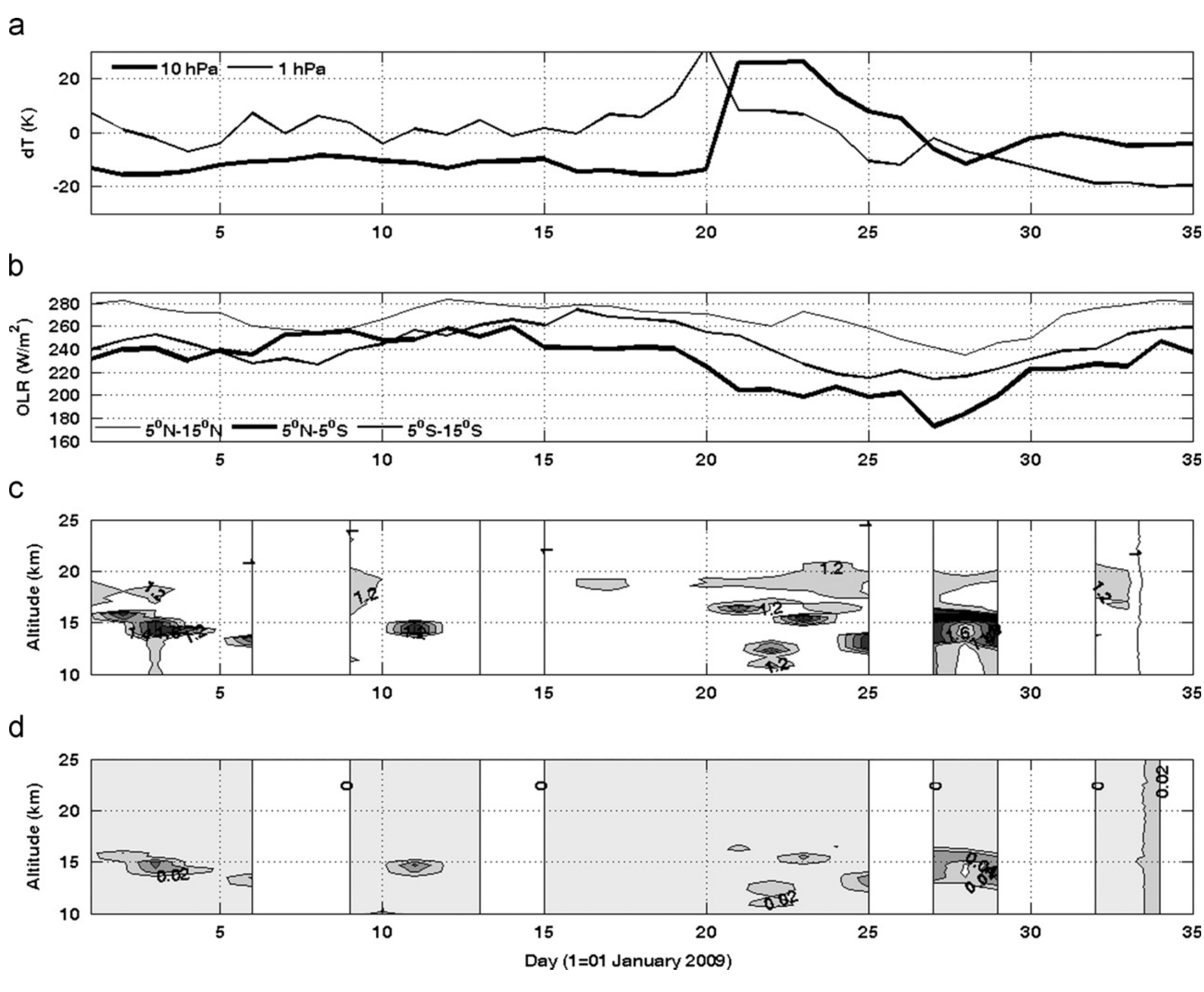


**Fig. 1.** (a) Time variation of zonal mean temperature difference between the latitudes 90°N and 60°N at 10 and 1 hPa, (b) time variation of daily OLR averaged for 70°E–90°E for the latitudes 5°N–5°S, 5°S–15°S and 5°N–15°N, (c) and (d) altitude-time cross section of scattering ratio and linear depolarization ratio respectively over Gadanki, for the day numbers 1–35 of January 2009. The white blocks in (c) and (d) denote data gaps.

which is $\beta_z(z)/\beta_m(z)$. Thus for an aerosol free Rayleigh atmosphere, SR is unity and with increasing aerosol concentration SR increases. In the present paper, SR of 1.25 is taken as a threshold for identifying cirrus days (Kulkarni et al., 2008).

### 2.3. ERA-Interim data

In the present paper, we use ERA-Interim winds, which are availabe for the 37 pressure levels from the surface to 1 hPa (Berrisford et al., 2009). This is the latest ECMWF global atmospheric reanalysis of the period 1989 to present. These data were prepared by European Center for Medium Range Weather Forecasting using their variational data assimilation system. The ERA-Interim data set consists of analysis conducted at six-hour intervals available for a 1.5° latitude–longitude grid and for 37 standard pressure levels from the surface to 1 hPa. More details about the data sets can be obtained from the ECMWF website (http://www.ecmwf.int/research/era/do/get/index).

## 3. Results

The state of high-latitude winter hemisphere during January–February 2009 is depicted in Fig. 1a using ERA-Interim data. During the beginning of January 2009, normal winter conditions can be observed with poleward decrease in temperature inferred from the negative polar temperature gradient and prevailing eastward winds at polar latitudes. However, a major SSW event occurred during January 21–27, which can be identified from the positive polar temperature difference associated with the reversal of winds from eastward to westward at 10 hPa. According to Manney et al. (2009), the 2009 SSW event is a remarkable and characterized by a splitted polar vortex. The stratopause dropped dramatically and broke down, then reformed at very high (75–80 km) altitude. Fig. 1b shows the daily variation of outgoing long-wave radiation (OLR) averaged for 70°E–90°E for the latitudes 5°N–5°S, 5°S–15°S and 5°N–15°N. The OLR data are obtained from the National Oceanic and Atmospheric Administration (NOAA) operational satellites. The OLR has been used as a proxy for the intensity of convection in the tropics; lower values of OLR correspond to more enhanced convective activity. For example, the OLR which is less than 240 W/m$^2$ is a general indicator of precipitation in the tropics (e.g., Lau and Chan, 1983). The daily variation of OLR averaged for the longitudes 70°E–90°E and equatorial region shows that the OLR decreases coinciding with the onset of the warming event. The equatorial OLR begins to decrease drastically from 240 to 200 W/m$^2$ from day number 19 to 21. It further decreases to 170 W/m$^2$ 27 January 2009 followed by an increase. The equatorial northern and southern hemispheric OLR also decrease during the warming event with minimum values of 230 W/m$^2$ and 215 W/m$^2$. During the period of reduced OLR, which shows deep convection, the scattering ratio estimated from the Mie-lidar observations shows large values indicating the occurrence of cirrus clouds (Fig. 1c). The scattering ratio shows larger variabilities at 15 km with values greater than 6 on day numbers 27 and 29, whereas the cirrus cloud is not present on day number 28. Wang et al.'s (1996) results based on Stratospheric Aerosol and Gas Experiment (SAGE) II data suggested that thin cirrus preferred to occur mostly at an altitude of 15 km over the equator. The dual polarization (co- and cross-) measurements of the backscattered signal can be used to determine the relative concentrations of water and ice in the clouds. Since the ice particles are different in their orientation, shape and size, they cause corresponding changes in the depolarization value. The depolarization value, which is conventionally used to identify the composition of the cloud, can

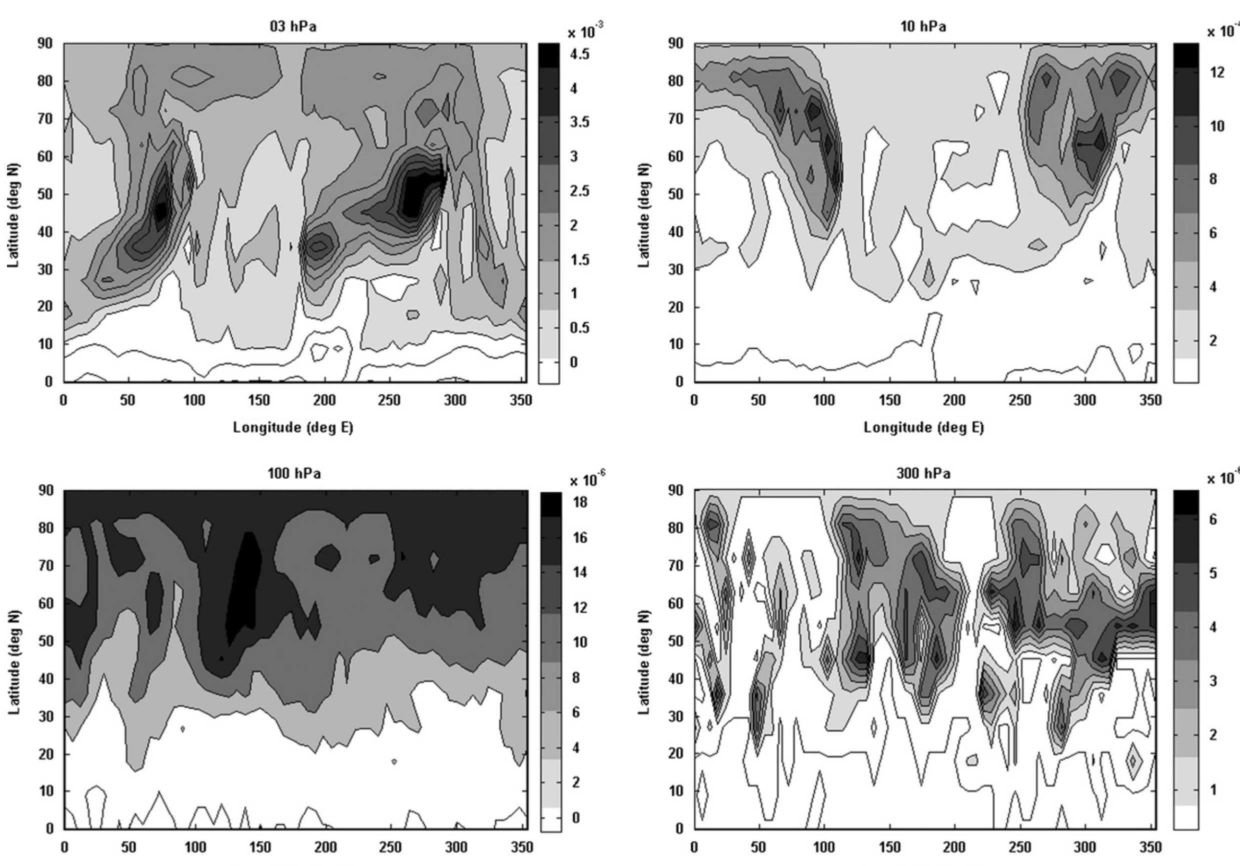


**Fig. 2.** Latitude–longitude cross section of Potential vorticity (km$^2$ kg$^{-1}$ s$^{-1}$) on 23 January 2009 at different pressure levels 03, 10, 100 and 300 hPa.

be expressed as the product of the scattering ratios of the cross-polarized and the co-polarized components of the backscattered signal and the lidar ratio, which is taken as 0.014 (Sivakumar et al., 2003). The depolarization ratio (bottom panel of Fig. 1) also shows similar variability. When scattering ratio is more, the depolarization ratio is also more indicating the presence of ice crystals. These results reveal that the high latitude SSW event influences the occurrence of cirrus clouds.

In order to explain the relationship between the SSW and equatorial OLR, we consider latitude–longitude cross section of potential vorticity (PV) at different pressure levels from 03 to 600 hPa in Fig. 2. At 3 hPa, the latitude–longitude PV map on 23 January 2009 shows two tongues of high PV emanating from polar latitudes and extending down to equator and westward in the longitude range 0–100°E and 200–300°E. It may be noted the SSW event is a splitted polar vortex event caused by 16-day planetary wave of wavenumber 2 (Manney et al., 2009; Sridharan et al., 2010). This extension is observed at all pressure levels not only in the stratosphere, but also in upper troposphere. At 200 hPa, the extension of PV even reaches 10° latitude at longitudes 60°E and 250°E. These PV maps give the evidence of some horizontal exchange between the tropical and polar latitudes. Even at pressure levels 300–500 hPa, weak extension of PV from polar to tropical region is observed. The PV intrusion in the stratosphere can drives a circulation, which will be continued into the tropical troposphere or the PV intrusion in the upper troposphere can affect Hadley circulation.

In order to see the difference in the circulation pattern before and during the SSW event, the ERA meridional and vertical winds are averaged for the days 1–7, 11–17 and 21–27 January 2009, which are taken as representatives of control, pre-warming, and warming days respectively. The mean winds for pre-warming days are subtracted from those of control days and the same for warming days are subtracted from those of pre-warming days. Fig. 3 shows the latitude-pressure cross section of change in zonal mean meridional velocity (top panels) and omega (bottom panels) for pre-warming (left panels) and warming (right panels) days. From the equation of omega (Holton, 2004), we can infer that positive vorticity advection with no thermal advection or warming advection results in a negative omega, that is, ascending motion. Similarly, negative vorticity advection or cold advection results in a positive omega corresponding to descending motion. It may be observed that during the period of the SSW event, the zonal mean poleward circulation shows a slight enhancement at 31–38 km (10–3 hPa) and 12–14 km (200–150 hPa) and During pre-warming, the change in vertical winds is negative indicating increase in the upward or decrease in the downward winds are observed at tropical latitudes, except around 10°S and 10°N. During warming days, there is shift in the region of increase in the upward (or decrease in the downward) winds. More upward winds are noticed at an extended latitude region with one around equator (5°N–15°S) and other at latitudes 15°N–45°N and downward winds are observed at latitudes 5°N–15°N. The enhancement of upward winds in the latitude region 15°N–40°N could be due to warm advection of air mass from polar latitudes. Besides, the change in meridional circulation at 12–14 km (150–200 hPa) is positive during warming days indicating weakening of the winds at 100 and 300 hPa and strengthening in between and the Hadely cell shifts upwards at latitudes south of 15°N, These results suggest that the SSW induces large upward and northward circulation over equatorial upper tropospheric region.

The time-altitude cross section of radiosonde observed RH, temperature, zonal and meridional winds are plotted in Fig. 4 for

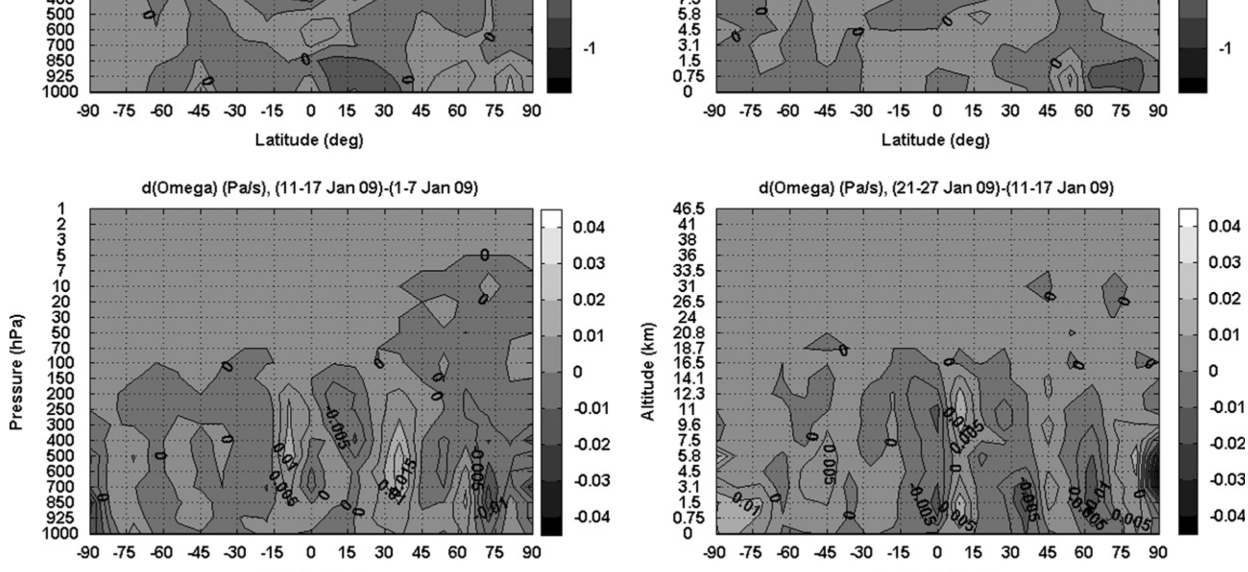


**Fig. 3.** Latitude–pressure cross section of change in zonal mean meridional velocity (top panels) and omega (bottom panels) for pre-warming (left panels) and warming (right panels) days. The pressure levels are converted into approximate heights and are given as vertical coordinate in the right panels for reference.

the day numbers 1–59 starting from 01 January 2009. The eastward winds prevailing at altitudes below the tropopause intensify just before the warming, but change to large westward winds after the warming. Consistent with the ERA-Interim meridional winds, the radiosonde meridional winds also show intense northward winds during and a few days after the warming event. Before the onset of the SSW event, the maximum RH in the altitudes 11–15 km is around 20%. Immediately after the onset of the SSW event, the RH values in the altitude range 11–15 km over Gadanki increase even to 45–50% and 30–45% in the height range 11–13 km, during 22–23 and 25–27 January 2009, respectively. The tropopause temperature is observed to be colder during the SSW event. The daily variation of cold point tropopause temperature, its height and integrated water vapour shown in Fig. 5 reveals clearly that though the cold point tropopause temperature show variabilities in the time scale of 4–6 days before the onset of the major SSW event, it remains nearly constant around 188 K during day numbers 18–31, which includes the major SSW event. There is a slight warming (189 K) on days 27 and 29. The ERA 100 hPa temperature at 9°N averaged for 70°E–90°E shows colder temperature during the SSW event and the temperature suddenly increases by 5 K on day numbers 28 and 29. The zonal mean ERA temperature at 9°N also shows decrease of tropopause temperature from day number 16 to 27 and the temperature slightly increase on day numbers 28–32, though it is not trivial that the zonal mean should show the same behaviour as the station data. The tropopause height is also around 17 km during day numbers 21–26. The integrated water vapour for the altitude region surface to 40 km shows a drastic increase from 7% on day number 24 to 23% on day numbers 27 and 28.

## 4. Discussion

The present study reports changes in the tropical troposphere during a major warming event, which occurred during the end of January 2009 due to circulation changes caused by the warming. The ERA observations of zonal mean meridional winds show an increase in the northward circulation at upper tropospheric heights during the SSW event. The vertical winds are upward near south of equator and downward at latitudes 20°N at pressure levels 1000–200 hPa before the warming event and they are changed into large upward over equatorial region during the warming event. The radiosonde observations over Gadanki (13.5°N, 79.2°E) show the presence of ~40% relative humidity at 11–13 km, lower tropopause temperature, enhancement of westward winds and northward winds in the altitude region 15–17 km during the SSW event. The OLR, a proxy for tropical convection, averaged over the longitudes 70°E–90°E, decreases coinciding with the onset of the warming event and shows a low value of 170 W/m$^2$ over equator (5°N–5°S) on day 27, indicating deep convective activity. As expected from the deep convection and increase in the humidity level, the Mie-lidar observations carried out at Gadanki (13.5°N, 79.2°E) shows the presence of cirrus cloud coinciding with the day of deep convective activity and its disappearance with the decrease in convective activity after the SSW event.

Earlier, an Eulerian model study of Garcia (1987) suggests that an interaction of rapidly varying planetary wave activity interaction with the background flow in the winter hemisphere and associated Eliassen–Palm flux divergence could lead to a clockwise cell in the entire stratosphere, which can extend to subtropics of the

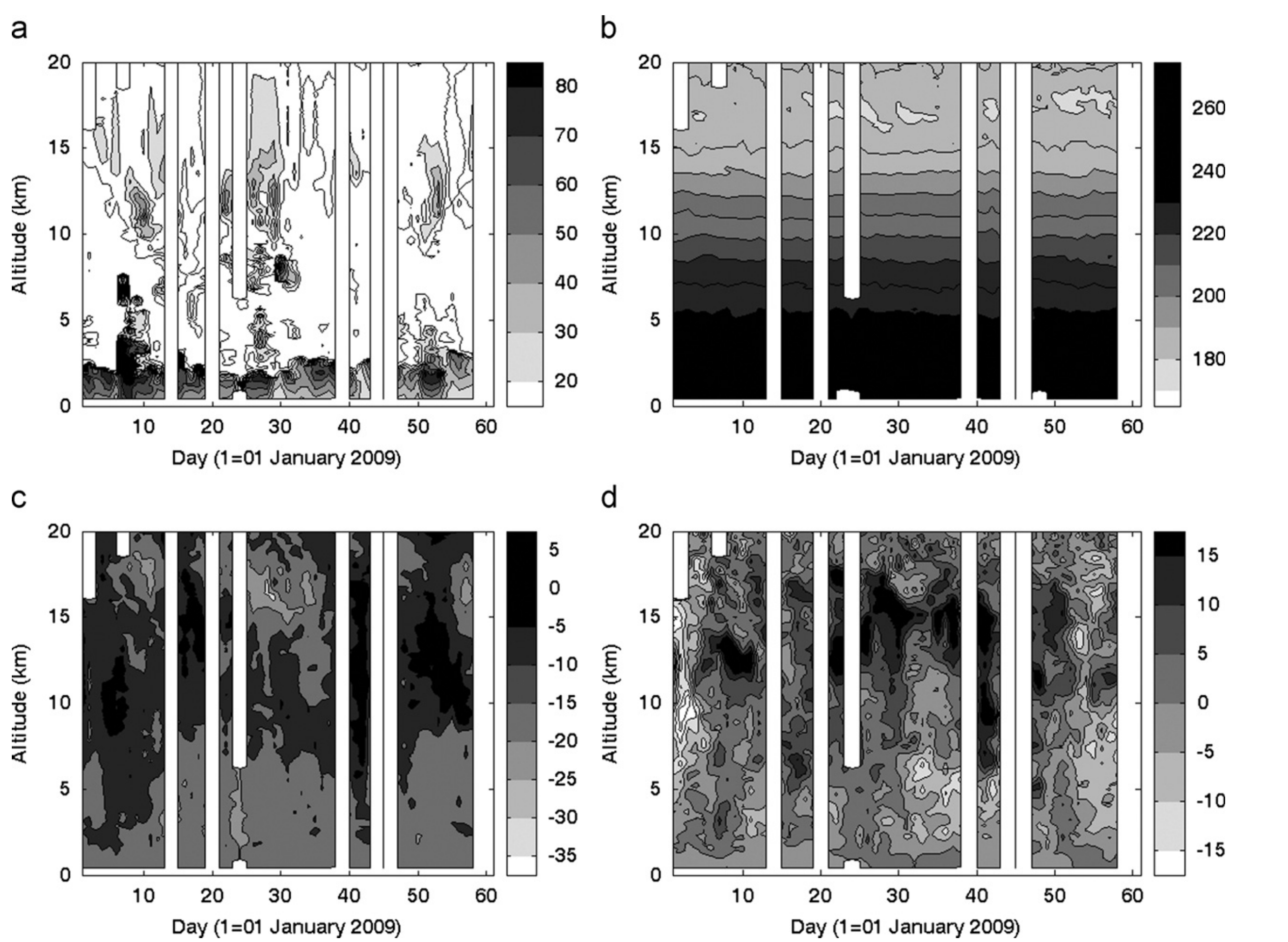


**Fig. 4.** Altitude-time cross section of (a) relative humidity (%), (b) temperature (K), (c) zonal wind (m/s) and (d) meridional wind (m/s) over Gadanki observed by radiosonde launched at Gadanki for the day numbers 1–59 starting from 01 January 2009.

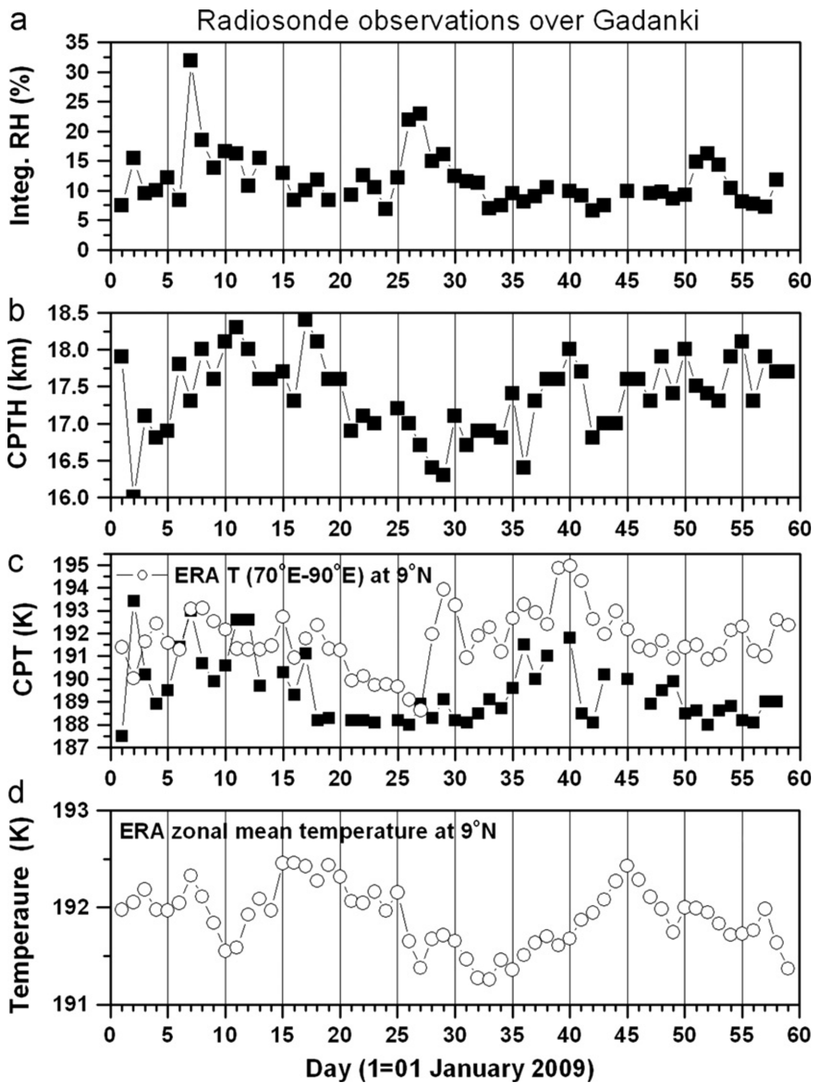


**Fig. 5.** (a)–(c) Daily variations of height integrated water vapour, cold point tropopause height, cold point tropopause temperature observed by radiosondes launched at Gadanki. The ERA temperature at 100 hPa averaged for 70°–90°E at 9°N and zonal mean temperature at 100 hPa at 9°N are also plotted in (c) and (d) for comparison.

summer hemisphere. Though, their model results did not include Hadley cell, their study demonstrates that the stratospheric circulation affects the tropospheric, even tropical, circulation due to the requirement of continuity. For the stratospheric and tropical circulation, Haynes et al. (1991) proposed a mechanism that stratospheric wave drag induces a meridional circulation which is closed with an opposite circulation in the surface level. Since the eddy flux is convergent in the extra-tropical stratosphere, it drives a downward motion in the region and it should be compensated by upward motion in the tropics and summer hemisphere. In the time-mean, the tropospheric circulation changes are directly under the stratospheric wave forcing. However, if the stratospheric wave forcing approaches the subtropics or if the forcing is a transient process, Plumb and Eluszkiewicz (1999) demonstrated that the changed upwelling even intrudes into the tropics and it could be one possible explanation for the change in the Hadley cell. Using potential vorticity, temporal evolution of the size, shape and orientation of the main circumpolar vortex can be studied, as shown in Dunkerton and Delisi (1986). The size of the vortex determines the range of latitudes over which planetary waves can propagate. The latitude–longitude cross section of potential vorticity shown in Fig. 2 of the present study clearly reveals the intrusion of the stratospheric wave driving into the subtropics, at least at 3 hPa. The other explanation would be that changed eddy fluxes in the troposphere affect the Hadley cell. It means that the eddies that usually propagate meridionally to the tropospheric subtropics, now propagate upwards to the stratosphere. This means that they are absent in the tropospheric subtropics.

Collimore et al.'s (2003) study showed that in the tropics, the QBO westward winds in the lower stratosphere could cause the tropopause to be higher than normal, allowing convection to penetrate deeper than normal. The deeper clouds, which tend to have larger diameters than shallower clouds, lead to more convergence of mass, moisture, and energy at low levels, precipitating the formation of more convective clouds. As the stratospheric QBO winds are in the eastward phase during January 2009, the stratospheric QBO is unlikely to influence the tropospheric convective activity in the present case.

Earlier observations have shown that the sudden warming enhances upwelling in the equatorial southern hemisphere but reduces upwelling in the northern hemisphere (Eguchi and Kodera, 2007). However, the results presented here show that upwelling is induced in both equatorial northern and southern hemispheric regions for the January 2009-warming. The convergence of the water vapour over equator enhances convective activity and upward motion. Thus anomalous meridional circulation in the equatorial troposphere develops with time together with the change in water vapour content in the lower level during the SSW event.

The occurrence rate of cirrus is normally less during winter, when compared to other seasons (Kulkarni, 2009). Our observations show persistent occurrence of cirrus clouds during when the SSW event occurs at high-latitudes. The major SSW event induces large upward winds and deep convection and low temperature, which may eventually cause the cirrus cloud formation in the tropical troposphere. The cirrus clouds are also formed by the low temperature due to the upward motion in the upper troposphere and also due to moist air ascending to the upper troposphere. This can be noted in our observations that there is strong enhancement in the RH value after the day number 25, coinciding with the enhancement in the scattering ratio. Once the convective activity becomes weak about a week after the warming event, the cirrus clouds disappear and the temperature around the tropopause increases.

Based on the results of Boehm et al. (1999), they hypothesized that a source of large-scale upward motion must be present to maintain tropical cirrus. Besides, Boehm and Verlinde (2000) noted in their radiosonde observations that cirrus cloud occurrence coincided with the cold phase of the Kelvin waves, which were showing downward phase propagation from the lower stratosphere into the upper troposphere. In our observations, when cirrus clouds are formed, the tropopause temperature does not show any planetary wave variability and it remains almost constant around 188 K. It suggests that planetary waves are unlikely to play a role in the formation of the observed cirrus clouds during this SSW event. Optically thin cirrus layers in the upper troposphere are thought to form through two mechanisms, namely, spreading and decay of the outflow from deep convection (Prabhakara et al., 1993) and in situ through cooling associated with large-scale rising motion (Winker and Trepte, 1998). Consistent with the model results of Boehm et al. (1999), our observations suggest that large-scale rising motion because of air mass intrusion from high latitudes to equator in the upper tropospheric region as observed in the present study during SSW days may be responsible for the low OLR and persistence of cirrus clouds for many days.

## Acknowledgements

*Interpolated OLR data were provided by the NOAA/OAR/ESRL PSD, Boulder, Colorado, USA, from their Website at* http://www.esrl.noaa.gov/psd/. The ECMWF ERA data used in the present study were provided by BADC and downloaded from their website http://data-portal.ecmwf.int/data/d/interim_daily. The authors would like to acknowledge the SAFAR program of NARL. They also gratefully acknowledge the help rendered by supporting staff in conducting lidar and radiosonde observations. They would like to thank the Editor and the Reviewer for their comments and suggestions, which greatly helped to improvise the manuscript.

## References

Berrisford, P., Dee, D., Fielding, K., Fuentes, M., Kallberg, P., Kobayashi, S., Uppala, S., 2009. The ERA-Interim Archive. European Centre for Medium Range Weather Forecasts, Shinfield Park, Reading, Berkshire RG2 9AX, United Kingdom 1–16.

Boehm, M.T., Verlinde, J., Ackerman, T.P., 1999. On the maintenance of high tropical cirrus. Journal of Geophysical Research 104, 24423–24433.

Boehm, M.T., Verlinde, J., 2000. Stratospheric influence on upper tropospheric tropical cirrus. Geophysical Research Letters 27, 3209–3212.

Collimore, C.C., Martin, D.W., Hitchman, M.H., Huesmann, A., Waliser, D.E., 2003. On the relationship between the QBO and tropical deep convection. Journal of Climate 16, 2552–2568.

Dunkerton, T.J., Delisi, D.P., 1986. Evolution of potential vorticity in the winter stratosphere of January-February 1979. Journal of Geophysical Research 91, 1199–1208.

Eguchi, N., Kodera, K., 2007. Impact of the 2002, Southern Hemisphere, stratospheric warming on the tropical cirrus clouds and convective activity. Geophysical Research Letters 34, L05819. doi:10.1029/2006GL028744.

Fernald, F.G., 1984. Analysis of atmospheric lidar observations: some comments. Applied optics 23, 652–653.

Fritz, S., Soules, S.D., 1970. Large-scale temperature changes in the stratosphere observed from Nimbus-III. Journal of the Atmospheric Sciences 27, 1091–1097.

Garcia, R.R., 1987. On the mean meridional circulation of the middle atmosphere. Journal of the Atmospheric Sciences 44, 3599–3609.

Haynes, P.H., Marks, C.J., McIntyre, M.E., Shepherd, T.G., Shine, K.P., 1991. On the downward control of extratropical diabatic circulation by eddy induced mean zonal forces. Journal of the Atmospheric Sciences 48, 651–678.

Holton, J.R., 2004. fourth ed.An Introduction to Dynamic Meteorology, 88. Elsevier Academic Press, p. 165.

Klett, J.D., 1985. Lidar inversion with variable backscatter/extinction ratios. Applied Optics 24, 1638–1643.

Kodera, K., 2006. Influence of stratospheric sudden warming on the equatorial troposphere. Geophysical Research Letters 33, L06804. doi:10.1029/2005GL024510.

Kodera, K., Yamada, K., 2004. Impact of the SH major stratospheric warming on the Hadley circulation: a case study. Papers in Meteorology and Geophysics 54 (3–4), 115–120.

Kulkarni, P., Ramachandran, S., Bhavani Kumar, Y., Narayana Rao, D., Krishnaiah, M., 2008. Features of upper troposphere and lower stratosphere aerosols observed by lidar over Gadanki, a tropical Indian station. Journal of Geophysical Research 113, D17207. doi:10.1029/2007JD009411.

Kulkarni, P., 2009. Investigation of aerosols and cirrus in the upper troposphere and lower stratosphere, Ph.D. Thesis, Sri Venkateswara University, Tirupati, India.

Lau, K.M., Chan, P.H., 1983. Short-term climate variability and atmospheric teleconnections from satellite-observed outgoing longwave radiation. I: simultaneous relationships. Journal of Atmospheric Sciences 40, 2735–2750.

Manney, G.L., Schwartz, M.J., Krüger, K., Santee, M.L., Pawson, S., Lee, J.M., Daffer, W.N., Fuller, R.A., Livesey, N.J., 2009. Aura Microwave Limb Sounder observations of dynamics and transport during the record-breaking 2009 Arctic stratospheric major warming. Geophysical Research Letters 36, L12815. doi:10.1029/2009GL038586.

Matsuno, T., 1971. A dynamical model of the stratospheric sudden warming. Journal of Atmospheric Sciences 28, 1479–1494.

Nath, D., Ratnam, M.V., Patra, A.K., Murthy, B.V.K., Rao, S.V.B., 2010. Turbulence characteristics over a tropical station Gadanki (13.5°N, 79.2°E) estimated using high resolution GPS radiosonde data. Journal of Geophysical Research 115, D07102. doi:10.1029/2009JD012347.

Prabhakara, C., Kratz, D.P., Yoo, J.–M., Dalu, G., Vernekar, A., 1993. Optically thin cirrus clouds: radiative impact on the warm pool. Journal of Quantitative Spectroscopy and Radiative Transfer 49, 467–483.

Plumb, R.A., Eluszkiewicz, J., 1999. The Brewer–Dobson circulation: dynamics of the tropical upwelling. Journal of the Atmospheric Sciences 56, 868–890.

Ramachandran, S., Jayaraman, A., 2003. Balloon-borne study of the upper tropospheric and stratospheric aerosols over a stropical station in India. Tellus 55B, 820–836.

Sridharan, S., Raghunath, K., Sathishkumar, S., Nath, D., 2010. First results of warm mesospheric temperature over Gadanki (13.5°N, 79.2°E) during the sudden stratospheric warming of 2009. Journal of Atmospheric and Solar-Terrestrial Physics, 72. doi:10.1016/j.jastp.2010.06.003.

Sivakumar, V., Bhavanikumar, Y., Rao, P.B., Mizutani, K., Aoki, T., Yasui, M., Itabe, T., 2003. Lidar observed characteristics of the tropical cirrus clouds. Radio Science 38 (6), 1094. doi:10.1029/2002RS002719.

Thuburn, J., Craig, G.C., 2000. Stratospheric influence on tropopause height: the radiative constant. Journal of the Atmospheric Sciences 57, 17–28.

Wang, P.–H., Minnis, P., McCormic, M.P., Kent, G.S., Skeens, K.M., 1996. A 6-year climatology of cloud occurrence frequency from Stratospheric Aerosol and Gas Experiment II observations (1985–1990). Journal of Geophysical Research 101, 29407–29429.

Winker, D.M., Trepte, C.R., 1998. Laminar cirrus observed near the tropical tropopause by LITe. Geophysical Research Letters 25, 3351–3354.

Yulaeva, E., Holton, J.R., Wallace, J.M., 1994. On the cause of the annual cycle in tropical lower stratospheric temperature. Journal of the Atmospheric Sciences 51, 169–174.